American Journal of Applied Sciences

Original Research Paper

# Photoelectrochemical Corrosion of GaN/AlGaN-Based p-n Structures

**[1,2]Alexander Usikov, [1]Heikki Helava, [3]Alexey Nikiforov, [4]Michael Puzyk, [1]Boris Papchenko and [1,5]Yuri Makarov**

*[1]Nitride Crystals Inc., 181 E Industry Ct., Ste. B, Deer Park, NY 11729, USA*
*[2]University ITMO, Kronverkskiy pr. 49, St. Petersburg 197101, Russia*
*[3]Boston University, Photonics Center, 8 St. Mary's St., Boston, MA 02215, USA*
*[4]Herzen University, Nab. r. Moyki 48, St. Petersburg 194186, Russia*
*[5]Nitride Crystals Group Ltd., 27 Engels av., St Petersburg 194156, Russia*

*Article history*
Received: 31-10-2015
Revised: 18-07-2016
Accepted: 30-07-2016

Corresponding Author:
Alexander Usikov
Nitride Crystals Inc., 181 E Industry Ct., Ste. B, Deer Park, NY 11729, USA and University ITMO, Kronverkskiy pr. 49, St. Petersburg 197101, Russia
Tel: +1 631 242 8853
Fax: +1 631 242 8906
Email: alexander.usikov@nitride-crystals.com

**Abstract:** Direct water photoelectrolysis using III-N materials is a promising way for hydrogen production. GaN/AlGaN based p-n structures were used as working electrodes in a photoelectrochemical process to investigate the material etching (corrosion). The structures were grown on sapphire substrates by chloride Hydride Vapor Phase Epitaxy (HVPE). First, the etching process occurs near vertically via channels associated with defects in the structure and penetrates deep into the structure. Then, the process involves etching of the n-type AlGaN barrier and n-GaN active layer in lateral direction resulting in formation of voids and cavities. The lateral etching is due to net positive charges at the AlGaN/GaN interfaces arising because of spontaneous and piezoelectric polarization in the structure and positively charged ionized donors in the space charge region of the p-n junction.

**Keywords:** Hydride Vapor Phase Epitaxy, III-N Structures, Photo-Assisted Electrochemical Process

## Introduction

Hydrogen is considered a candidate as the substantial energy carrier. In the process of hydrogen energy consumption, water, as the product of hydrogen oxidation, is harmless to the environment. Water exists profusely on earth and is a resource for hydrogen production. At present, several technologies are used or being developed for hydrogen generation using solar energy directly or indirectly. They include among others thermochemical water decomposition process driven by a concentrated solar system, generation of hydrogen through biomass, hydrogen production through photosynthetic microorganisms and hydrogen production by electrolysis (Turner *et al*., 2008). In the latter case the electrolysis can be driven by renewable electricity and performs water decomposition electrochemically.

Direct water photoelectrolysis is a promising way for hydrogen production. In this process, a semiconductor material immersed in an aqueous solution of electrolyte allows decomposition of water into $H_2$ and $O_2$ gases by solar irradiation of its surface. The required energy to split water molecules is generated by sunlight absorption in the semiconductor. The solar water splitting process may be spontaneous under illumination if the electrochemical redox potentials of Oxygen Evolution Reaction (OER) and Hydrogen Evolution Reaction (HER) in an electrolyte are exceeded by the energy gap of the semiconductor. This is fulfilled for GaN-based materials (Waki *et al*., 2007; Ohkawa *et al*., 2013; Chen and Wang, 2012; Aryal *et al*., 2010).

Not all of the electron-hole pairs generated in the semiconductor under illumination in an electrolyte can participate in OER and (or) HER. Carrier recombination at the surface and in the bulk of the layer reduces the gas generation rate. Another process having a negative effect on the gas evolution reaction is photo-corrosion or etching of the electrode material (Wolff *et al*., 2005). The corrosion is an issue for n-type materials as a photoelectrode because upward band-bending at the photoelectrode/electrolyte interface promotes photo-generated holes to transfer to the electrolyte. The holes at the interface not only oxidize water (OER) but oxidize the photoelectrode. On the other hand, in p-type

materials the band-bending promotes photo-generated electrons to transfer to the electrolyte where they participate in the HER process that almost leaves intact the surface of the photo-electrode chemically (Aryal *et al*., 2010; Rajeshwar, 2008; Liu *et al*., 2012). The p-type III-N materials as photoelectrodes have been less investigated in the photo-electrochemical process.

A direct water photoelectrolysis feature is a relatively low photocurrent density, up to tens mA/cm$^2$, because of relatively weakly concentrated sunlight used to illuminate the photoelectrodes. The typical values of the concentration factor range from 1× to 20×. Higher values of the concentration factor require a solar tracking system, resulting in electrolyte heating and necessitating an efficient heat sink. This does not comply with the concept of a simple design and low-cost usually requested from a photoelectrolysis system.

In this study we use as working electrodes GaN/AlGaN p-n structures with p-type GaN layer on the surface to investigate the material corrosion of the photoelectrochemical process. The structure was grown on a sapphire substrate by chloride Hydride Vapor Phase Epitaxy (HVPE).

## Materials and Methods

Several 8-10 μm-thick AlGaN/GaN p-n structures were grown by chloride HVPE on c-plane 2-inch sapphire substrates in a conventional horizontal-flow reactor. The growth procedure included in-situ sapphire substrate treatment followed by multilayer structure growth consisting of AlN/ $Al_xGa_{1-x}N$ (x~0.6) buffer layer and 4 pairs of $Al_xGa_{1-x}N$ (x~0.1-0.15)/$Al_xGa_{1-x}N$ (x~0.03-0.08) Stress Control Layers (SCL) on a sapphire substrate. The p-n structure was grown on the top of the SCL in the same run. The basic structure included a 50-100 nm-thick GaN active region co-doped by Zn and Si to have emission at 420 nm (Usikov *et al*., 2003), which was sandwiched between p- and n- $Al_xGa_{1-x}N$ barriers (x~0.05-0.12), all grown on a 2-3 μm thick n-GaN:Si contact layer (n~2-4×10$^{18}$ cm$^{-3}$). A 0.5-1 μm-thick p-type GaN contact layer doped with Mg covers the structure. The Mg doping resulted in p-type conductivity on the surface with a net acceptor concentration ($N_A$-$N_D$) up to (2-4) ×10$^{18}$ cm$^{-3}$ as determined by C-V characterization using Hg probe. Details of the structure growth and characterization can be found elsewhere (Kurin *et al*., 2014). Note that it was the p-type GaN layer surface that served as a photo-electrode (working electrode) in this study.

The 2-inch grown samples were immersed in a potassium hydroxide water electrolyte (5.7 weight % of KOH, pH = 14) under external electrical bias of +2.5 V and under solar irradiation. As a counter electrode a 2-inch diameter Ni plate was positioned parallel to the working electrode at a distance of about 3 cm. The GaN-based electrode was irradiated by a 150 W Xe lamp (AM 1.5 standard spectrum) with a concentration factor of 20×. The irradiated area (spot size) was adjusted to 1.3 inch (33 mm) diameter. The electrical contact to the sample (working electrode) was made through a spring clamp with indium pads. The structures were partly immersed in the electrolyte. A segment of the structure, which was used to hang the whole wafer by the clamp, was above the electrolyte to avoid a short circuit. The whole process of photoelectrolysis took about 6 min.

After that the samples were cleaved and their surface morphology and luminescence properties were examined in both top-view and cross-sectional configurations by high-resolution Scanning Electron Microscopy (SEM) and Cathodoluminescence (CL) spectroscopy and monochromatic CL imaging, respectively. The CL measurements were performed on a Gatan MonoCL2 system. CL spectra from three distinct areas of the samples described above were acquired by rastering a 10 kV electron beam over an area of 20×15 μm. For CL spectra from cross-sections, a 8 nA beam current was used. For CL spectra from the top surface, a slightly smaller beam current of 4 nA was used to mitigate electron beam induced charging on the top surface.

## Results

After the experiment, three areas can be seen on the structure surface by naked eye: (1) Area 1 that was not immersed into KOH, (2) Area 2 that was immersed into KOH but not illuminated by the Xe lamp and (3) Area 3 that was immersed into KOH and illuminated by Xe lamp. Area 3 on the surface of the structure appears to be dimmer than its surroundings.

Fig. 1a shows SEM images of cross sectional views of the same sample taken at Area 2 on the surface. All layers of the structure can be distinguished. The structure total thickness is about 9.5 μm. Note that in the experiment a +2.5 V bias was applied to the p-type top layer of the structure from external power source, i.e., the structure was a photo anode. During the experiment the measured value of photocurrent was found to decrease from 4.3 to 2.2 mA (0.5-0.25 mA/cm$^2$). Total thickness of the p-type layers is about 0.7 μm. No peculiarities that can be attributed to the photo-elecrochemical etching are observed. It seems that the value of photocurrent passing through Area 2 (the area that was immersed into the electrolyte but not illuminated by the Xe lamp) was too small to demonstrate a noticeable etching.

Fig. 1b shows a SEM image of the cross-sectional view of Area 3 of the same structure. All layers of the structure are the same as in Fig. 1a. However two rows

of micro-voids can be ascribed to the photo-elecrochemical etching. The position of the voids in the stack of layers in the structure makes it possible to assume that these voids are formed in the GaN active layer and in the underlying n-AlGaN barrier layer. The micro-voids can spread laterally and overlap leading to the formation of a large-size cavity. No apparent changes in the composition or elemental distribution of the constituent elements before and after etching were observed in the films as verified by results of energy-dispersive spectrometry.

Fig. 2 shows the large-size cavity that formed after the photoelctrolysis process performed on another AlGaN/GaN p-n structure but having higher photocurrent of 5.6-9.7 mA (0.65-1.1 mA/cm$^2$) under the same illumination. The large-size cavity may result in delamination of the p-layers from the structure. Fig. 3 shows a scanning micrograph of surface morphology in Area 3 of the sample in Fig. 1. Pits and large open cavities on the surface are attributed to the photo-electrochemical process. The pits density is about $2\times10^8$ cm$^{-2}$ and it varies over the sample surface up to (1-2)$\times10^9$ cm$^{-2}$ in the most defective areas near the microcracks. The CL spectra acquired from the sample surface have a weak emission at about 360 nm and a dominant broad peak centered around 420 nm as shown in Fig. 4a. The strongest luminescence was measured from the area illuminated by the Xe lamp (Area 3) where the density of nonradiative defects was likely decreased as a result of the photo-electrochemical etching. The coarser surface morphology in Area 3 may also improve the light extraction efficiency.

The dominant emission can be ascribed to the active layer located at a depth of 0.5-0.6 microns from the surface. Although the 10 kV beam penetration is limited to about 0.4 microns in depth (Yacobi and Holt, 1986), the electron beam spreading and various surface irregularities, such as pits and micro-cracks, allow beam electrons to reach active region located underneath the p-type contact layers and creates electron-hole pairs within the active layer. Their subsequent recombination results in an enhanced CL signal observed from the structure surface. A 1-3 μm thick Mg-doped p-type GaN layer grown in a separate run had a PL peak emission near 440 nm. Broad CL spectra overlap the emission from the p-GaN contact layer in Fig. 4.

To further elucidate the origin of the luminescence peaks, the CL spectra were acquired from cross-sections from the three distinct areas defined above. The spectra are shown in Fig. 4b. A strong broad emission from the active region at 414-420 nm is complemented by a strong signal from n-GaN contact layer at around 360 nm. Emission in the range of 324 to 331 nm could be ascribed to the AlGaN barriers. The rastered area included the substrate for reference purposes, for example, for a proper identification of the substrate-SCL layer interface in the monochromatic CL mapping.

The cross-sectional monochromatic CL maps acquired at the corresponding wavelengths of 324-331 nm and 420 nm for both samples are shown in Fig. 5. The maps at 324-331 nm and at 360 nm for both samples are very similar as they indicate that the corresponding luminescence emissions are coming from the AlGaN layers and from the GaN barriers in the bulk of the structure, respectively. The 420 nm emission corresponds to the GaN active region and is mainly localized within about a micron thick region near the top surface and correlates with subsurface void formation and top layer delamination in the area etched and illuminated by the Xe lamp (Area 3).

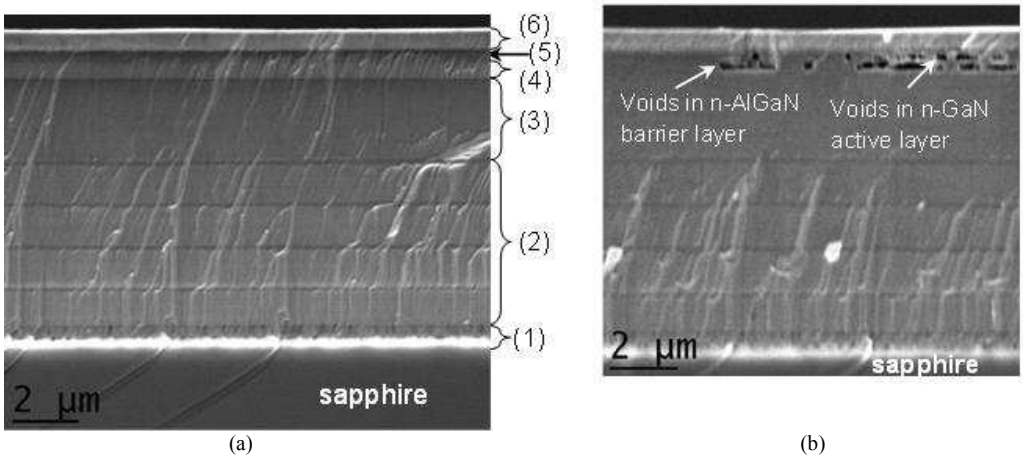


(a) (b)

Fig. 1. Cross-sectional SEM image of different areas of the AlGaN/GaN p-n structure after photo-electrolysis.(a) Area 2. No peculiarities related to the photo-electrochemical etching are observed. (1) AlN/AlGaN buffer, ~0.65 μm; (2) AlGaN/AlGaN four pairs, 4.97 μm; (3) n-GaN:Si contact layer, ~2.5 μm; (4) n-AlGaN barrier layer, ~0.5 μm; (5) GaN:(Zn+Si) active layer, ~0.2 μm; (6) p-GaN contact +p-AlGaN barrier layers, ~0.66 μm. (b) Area 3. Two rows of voids observed in the n- GaN active layer and in the n-AlGaN barrier lay are attributed to photo-electrochemical etching

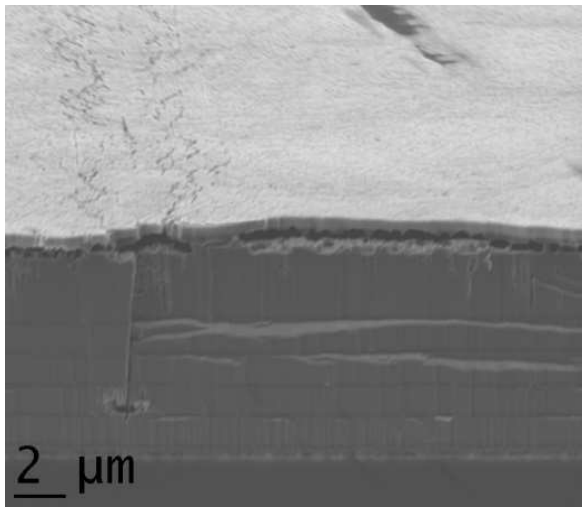


Fig. 2. Cross-sectional SEM image of Area 3 of another AlGaN/GaN p-n structure. Overlapped micro-voids that formed under higher photocurrent than in Fig. 2 sample off the p-layers from the structure created a large-size cavity that may delaminate or peel

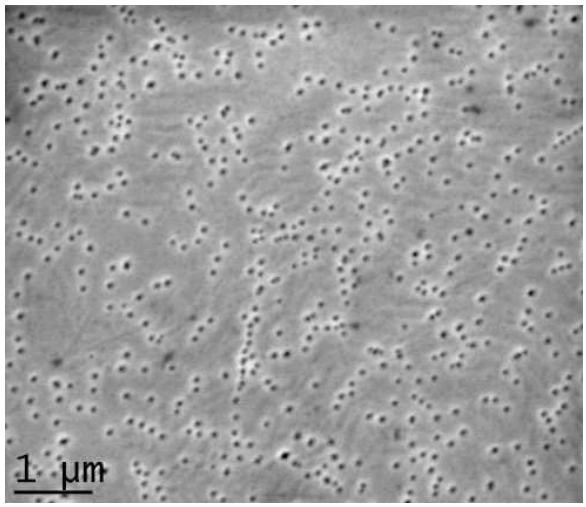


Fig. 3. SEM images of surface morphology after photo-electrochenical etching of AlGaN/GaN p-n structure in Fig. 1. Pits density is about $2\times10^{8}$ $cm^{-2}$

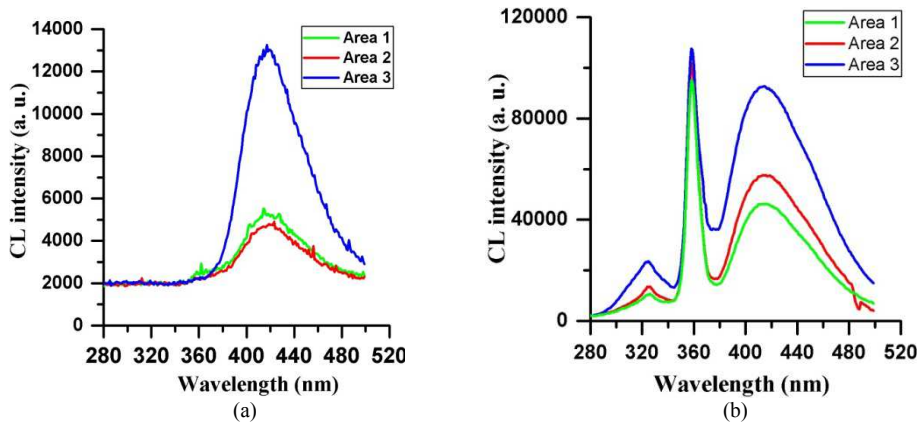


Fig. 4. CL spectra acquired from the sample surface (a) and from a cross section of the sample (b). Emission from the active region at ~420 nm is observed in both configurations

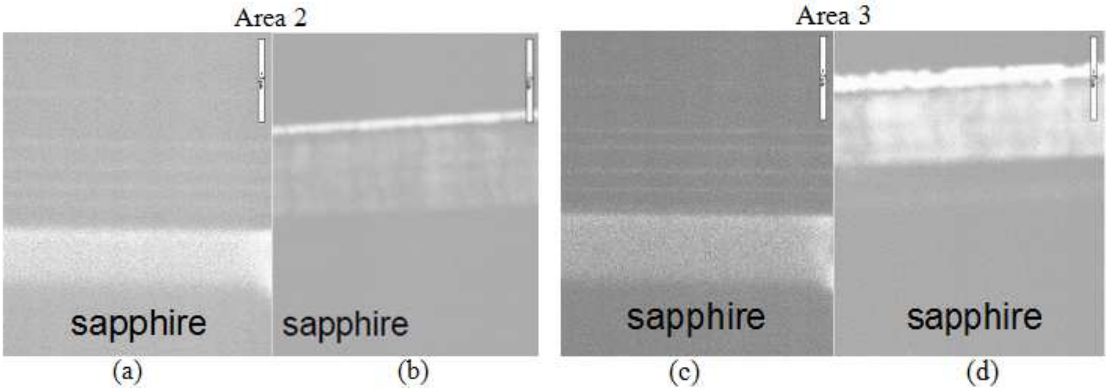


Fig. 5. Cross-sectional monochromatic CL maps after photo-electrochemical etching acquired at two areas at 324-331 nm (a, c); and 420 nm (b. d) for sample in Fig. 1. The scale bar is 5 μm

## Discussion

It was observed that photocurrent dropped in the first minute and become more or less stable later on at the experiment. Such behavior is typical for the electrochemical process with GaN-based electrodes (Aryal *et al*., 2010; Ohkawa *et al*., 2013) and can be associated with effectively decreasing of the electrode area that is contacting the electrolyte mainly due to the electrode corrosion and a production of gas microbubblers ($O_2$, $H_2$, $N_2$) that are result of the electrochemical process and can passivate the electrode surface. Obviously, the photoelectrochemical etching follows paths of the photo-current flow. The current flow paths in III-N GaN/AlGaN or GaN/InGaN materials, especially at low current, are nonuniform and can be associated with shunt conductivity in an extended defect system of grain boundaries, threading dislocations, local regions with irregular alloy composition enriched by metallic atoms (Ga or In) and others extended defects (Shmidt *et al*., 2015).

Voids observed in the SEM images in Figs. 2-3 suggest that the process of their formation proceeds in two stages. During the first stage, the etching process starts via channels (or shunts) in the extended defect system of the structure penetrating the p-type layers all the way into the underlying n-type layers. The shunts could be threading defects, grain boundaries and micro-cracks attributed to mosaic structure of the structures as-grown. During the second stage, the etching on the n-type AlGaN barrier and GaN active layer proceeds in a lateral direction resulting in the formation of voids and cavities underneath the p-type layers. Although the p-type layers of the structure remained unetched, the top surface exhibited a lot of pits.

The UV portion of the illumination light gets effectively absorbed in the p-GaN contact layer (at a depth of about 0.2-0.3 um from the surface) leading to the formation of excited electron-hole pairs. These pairs can be separated further by either the internal electric field of the space-charge region in the p-n junction of the structure when they drift towards it or by the specific band-bending at the p-GaN layer/electrolyte interface. The potential barrier at the p-n junction is higher than the bend-bending at the surface of the p-GaN layer and the separation of the excited electron–hole pairs could be further affected by p-n junction resulting in the generation of a photocurrent. The photo-generated carriers may participate in two competitive processes in the structure employed as an anode and immersed into an electrolyte under irradiation: (1) Oxygen Evolution Reaction (OER) and (2) photo-etching of GaN and GaN-based materials. However, because of a too thick p-GaN layer (0.5-0.6 μm thick) the excited electron-hole pairs recombine mostly at the structure surface and in the p-layer before being separated by the p-n junction producing as a result a relatively low photocurrent. It appears that relatively low photocurrent flows non-uniformly through the structure selecting paths with higher conductivity that are threading defects and micro cracks.

We speculate that photo-generated holes could assist in oxidative decomposition of p-GaN, primarily in the vicinity of the threading defects forming dangling bonds of $Al^{3+}$ and $Ga^{3+}$ atoms. Hydroxide ions ($OH^-$) from the electrolyte would then attack the $Al^{3+}$ and $Ga^{3+}$ dangling bonds and form hydroxides $Al(OH)_3$ and $Ga(OH)_3$ (Zhuang and Edgar, 2005; Macht *et al*., 2005). Dissolution of the hydroxides would lead to the formation of soluble $Al_2O_3$ and $Ga_2O_3$. Continuous formation and dissolution of the oxides in the solution would further simulate the etching process.

The etching process may move deeper into the layers via the threading defects. The Mg-doped p-type GaN and AlGaN layers have ionized $Mg^-$ acceptors and may screen partly the positive charge of the dangling bonds preventing the etching of the p-type layers but still allowing the etching to proceed along the threading

defects. Indeed we did not observe any appreciable etching of the top p-layers. However, some micro-cracks and numerous pits associated with etching were observed on the top surface as can be seen in Fig. 3. It is likely that these pits are associated with dislocations.

The step involving lateral etching in Figs. 1-2 can be explained considering effects resulting in a positive charge at layer interfaces. It is know that spontaneous and piezoelectric polarization between AlGaN/GaN layers in the structure results in a formation of a net positive charge at their interface (Mishra *et al*., 2002). Fig. 6 shows a net positive charge at the AlGaN/GaN interface in the AlGaN layer caused by the sum of the net spontaneous polarization and piezoelectric polarization between the AlGaN and GaN layers in the structure growing along the *c*-direction (Mishra *et al*., 2002). $Q_{\pi}$, AlGaN includes the contribution of spontaneous and piezo-electric contributions for AlGaN layer and $Q_{\pi}$, GaN is the only spontaneous polarization for the GaN layer as it has been assumed to be relaxed due to a much larger thickness than that of the AlGaN layer.

The positive $+Q_{\pi}$ charge at the bottom side of the thick GaN layer in Fig. 6a has a negligibly small effect on the charges at the AlGaN/GaN interface due to a presence of large number of electrons, traps and defects between the interface and the bottom portion of the thick underlying GaN layer. The sheet charge due to polarization in the AlGaN layer surface and at the interface is balanced also. To keep neutrality, the positive charge at the interface is compensated by electron accumulation forming a two Dimensional Electron Gas (2DEG) close to the interface (Mishra *et al*., 2002), the source of electrons in the 2DEG is the surface states (Ibbetson *et al*., 2000).

The structures in this study had a stack of doped GaN and AlGaN layers at the top (i.e., the n-GaN active layer was sandwiched between n- and p-AlGaN barrier layers) that influences the net positive charge compare to that depicted in Fig. 5. First of all, negatively charged ionized acceptors ($Mg^-$) in the p-AlGaN layer may screen positive polarization charge at the p-AlGaN barrier layer/n-GaN active layer interface. In addition, a thin n-GaN active layer is not fully relaxed and may have additional positive piezoelectric polarization charge at the n-GaN active layer/n-AlGaN barrier layer interface.

Then, n-AlGaN barrier also has a positive piezoelectric polarization charge at the interface with n-GaN contact layer beneath (Fig. 1a for reference to the structure design). Note also that all thin AlGaN layers having higher composition in the AlGaN/AlGaN four-pairs structure, beneath the n-GaN contact layer, have a net positive polarization charge. However these layers are located deep in the structure, further away from the structure surface. Only two thin n-GaN active and n-AlGaN barrier layers are near the p-type layers and have positive piezoelectric polarization charge. An additional positive charge at the layer interfaces can be connected with positively charged ionized donors, which are Si+ presumably, in a space charge region of the p (AlGaN)-n (GaN) junction. This positive charge is located in the n-GaN active region too. Our separate experiments on photoelectrolysis with GaN layers only demonstrated porous-like etching of 5-6 μm thick n-GaN layers through the layer to the substrate whereas in p-n GaN structures having a p-GaN layer on the top the etching process was terminated on the p-n junction.

The net positive charge at the GaN/AlGaN n-n and p-n interfaces promotes $OH^-$ ions from the electrolyte to form $Ga(OH)_3$ and (or) $Al(OH)_3$ hydroxides and the nitrogen vacancy sites and continue the etching process along the positive charge position forming lateral voids and large-size cavities.

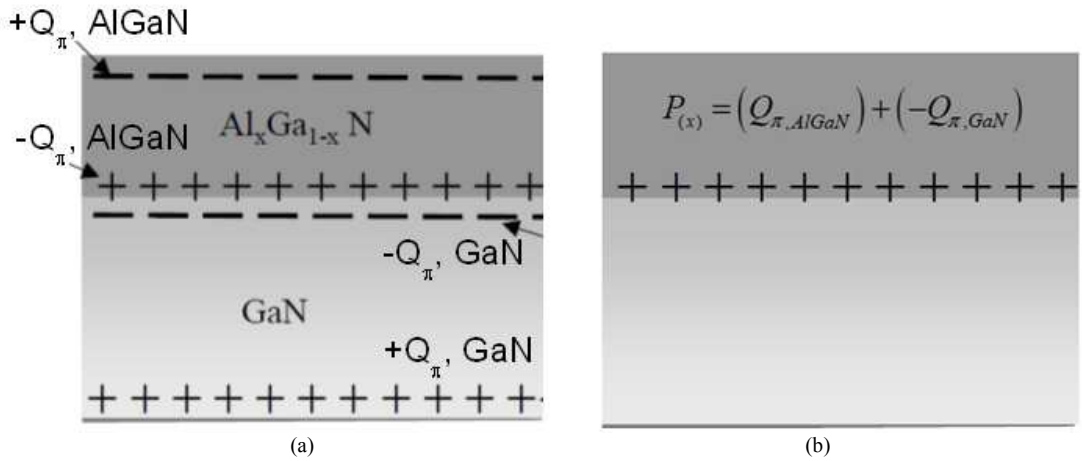


Fig. 6. CL Polarization charges in an AlGaN/GaN structure. (a) Charge polarization in individual layers of the structure (b) a net positive charge at the AlGaN/GaN interface in the AlGaN layer (Mishra *et al*., 2002)

When the etching process via threading defects reaches a layer with positive net charge it changes the etching direction from vertical to lateral presumably because of a stronger charge at the layer interface than that in the channel associated with threading defects and dangling bonds. When large threading defects, for example, large cracks are encountered the etching process may penetrate deeper into the structure as shown in Fig. 3b. However, the n-type AlGaN layer located at a depth from the surface switches the etching process from a vertical to a lateral direction due to a larger positive piezoelectric polarization charge at the layer interfaces.

Recent investigations of degradation mechanisms for similar HVPE-grown AlGaN/GaN p-n LED structures using multifractal analysis indeed demonstrated the existence of conductive paths (shunts) localized at threading defects (dislocations) (Shmidt *et al*., 2015). In our structures, the shunts are leakage paths for photo-currier flow that are responsible for non-uniform current spreading, diminishing the gas evolution reaction and decreasing the efficiency of direct water photoelectrolysis. Low-defect GaN-based working photoelectrodes are important for the photoelectrolysis process by focusing on gas generation but not etching.

## Conclusion

Two stages of photoelectrochemical etching under conditions of light illumination and external power source were observed in a GaN/AlGaN p-n structure having p-type layers on the top. During the first stage, the etching process occurs near vertically via channels associated with defects in the structure and penetrates deep into the structure to n-type layers passing p-type layers. The p-type layers of the structure remain unetched in the process. During the second stage, the process involves etching of the n-type AlGaN barrier and GaN active layer in a lateral direction resulting in the formation of voids and cavities beneath the p-type layers. The lateral etching is likely due to net positive charges at the AlGaN/GaN interfaces arising because of spontaneous and piezoelectric polarization in the structure and positively charged ionized donors in the space charge region of the p-n junction.

## Acknowledgement

Work at University ITMO was supported by the Ministry of Education and Science of Russian Federation (grant agreement 14.575.21.0054, unique identifier of research activities is RFMEFI57514X0054).

## Author Contributions

**Alexander Usikov:** Participation in the photoelctrolysis experiments, writing of the manuscript and give final approval of the version to be submitted and any revised version.

**Heikki Helava:** Design and select of the GaN/AlGaN p-n structures used in the experiments, reviewing of the manuscript for technical data and intellectual content.

**Alexey Nikiforov:** Acquisition of SEM and CL data and drafting of the manuscript.

**Michael Puzyk:** Participation in the photoelctrolysis experiments, analysis and interpretation of data.

**Boris Papchenko:** Design the work plan, organized the study and drafting of the manuscript.

**Yuri Makarov:** Growth of the GaN/AlGaN p-n structures by HVPE and Coordinated of the post-growth chatracterization of the structures.

## Ethics

This article is original and contains unpublished material. The corresponding author confirms that all of the other authors have read and approved the manuscript and no ethical issues involved.

## References

Aryal, K., B.N. Pantha, J. Li, J.Y. Lin and H.X. Jiang, 2010. Hydrogen generation by solar water splitting using p-InGaN photoelectrochemical cells. Applied Phys. Lett., 96: 052110-1-052110-3. DOI: 10.1063/1.3304786

Chen, S. and L.W. Wang, 2012 Thermodynamic oxidation and reduction potentials of photocatalytic semiconductors in aqueous solution. Chem. Mater., 24: 3659-3666. DOI: 10.1021/cm302533s

Ibbetson, J.P., P.T. Fini, K.D. Ness, S.P. DenBaars and J.S. Speck *et al*., 2000. Polarization effects, surface states and the source of electrons in AlGaN/GaN heterostructure field effect transistors. Applied Phys. Lett., 77: 250-252. DOI: 10.1063/1.126940

Kurin, S., A. Antipov, I. Barash, A. Roenkov and A. Usikov *et al*., 2014. Characterization of HVPE-grown UV LED heterostructures. Phys. Status Solidi, 11: 813-816. DOI: 10.1002/pssc.201300459.

Liu, S.Y., J.K. Sheu, M.L. Lee, Y.C. Lin and S.J. Tu *et al*., 2012. Immersed finger-type indium tin oxide ohmic contacts on p-GaNphotoelectrodes for photoelectrochemical hydrogen generation. Opt. Express, 20: A190. DOI: 10.1364/OE.20.00A190

Macht, L., J.J. Kelly, J.L. Weyher, A. Grzegorczyk and P.K. Larsen, 2005. An electrochemical study of photoetching of heteroepitaxial GaN: Kinetics and morphology. J. Crystal Growth, 273: 347-356. DOI: 10.1016/j.jcrysgro.2004.09.029

Mishra, U.K., P. Parikh and Y.F. Wu, 2002. AlGaN/GaN HEMTs: An overview of device operation and applications. Proc. IEEE, 90: 1022-1031. DOI: 10.1109/JPROC.2002.1021567

Ohkawa, K., W. Ohara, D. Uchida and M. Deura, 2013. Highly stable GaN photocatalyst for producing $H_2$ gas from water. Japanese J. Applied Phys., 52: 08JH04-08JH04. DOI: 10.7567/JJAP.52.08JH04

Rajeshwar, K., 2008. Hydrogen Generation from Irradiated Semiconductor-Liquid Interfaces. In: Solar Hydrogen Generation: Toward a Renewable Energy Future, Rajeshwar, K., R. McConnell and S. Licht (Eds.), Springer New York, ISBN: 978038772809-4, pp; 167-228.

Shmidt, N., E. Shabunina, A. Usikov, A. Chernyakov and S. Kurin *et al*., 2015. Peculiarities of defect generation under injection current in LEDs based on A3N nanostructure. Phys. Status Solidi, 12: 1136-1139. DOI: 10.1002/pssc.201400218

Turner, J., G. Sverdrup, M.K. Mann, P.C. Maness and B. Kroposki *et al*., 2008. Renewable hydrogen production. Int. J. Energy Res., 32: 379-407. DOI: 10.1002/er.1372

Usikov, A.S., D.V. Tsvetkov, M.A. Mastro, A.I. Pechnikov and V.A. Soukhoveev *et al*., 2003. Indium-free violet LEDs grown by HVPE. Phys. Status Solidi, 0: 2265-2269. DOI: 10.1002/pssc.200303521

Waki, I., D. Cohen, R. Lal, U. Mishra and S.P. Den Baars *et al*., 2007. Direct water photoelectrolysis with patterned n-GaN. Applied Phys. Lett., 91: 093519-093519. DOI: 10.1063/1.2769393

Wolff, N., M. Rapp and T. Rotter, 2005. Electrochemical etching and CV-profiling of GaN. Phys. Status Solidi, 2: 990-993. DOI: 10.1002/pssc.200460607

Yacobi, B.G. and D.B. Holt, 1986. Cathodoluminescence scanning electron microscopy of semiconductors. J. Applied Phys., 59: R1-R24. DOI: 10.1063/1.336491

Zhuang, D. and J.H. Edgar, 2005. Wet etching of GaN, AlN and SiC: A review. Mater. Sci. Eng.: R Rep., 48: 1-46. DOI: 10.1016/j.mser.2004.11.002